Research Article | Vol. 12, No. 5 / 1 May 2021 / Biomedical Optics Express 2586
Biomedical Optics EXPRESS

Laser-induced injury of the skin: validation of a computer model to predict thresholds

MATHIEU JEAN AND KARL SCHULMEISTER*

Seibersdorf Labor GmbH, Seibersdorf 2444, Austria
karl.schulmeister@seibersdorf-laboratories.at

Abstract: The exposure and emission limits of ICNIRP, IEC 60825-1 and ANSI Z136.1 to protect the skin are based on a limited number of *in-vivo* studies. To broaden the database, a computer model was developed to predict injury thresholds in the wavelength range from 400 nm to 20 µm and was validated by comparison with all applicable experimental threshold data (ED_{50}) in the wavelength range from 488 nm to 10.6 µm and exposure durations between 8 µs and 630 s. The model predictions compare favorably with the *in-vivo* data with an average ratio of computer prediction to ED_{50} of 1.01 (standard deviation ± 46%) and a maximum deviation of 2.6. This computer model can be used to improve exposure limits or for a quantitative risk analysis of a given exposure of the skin.

1. Introduction

Laser radiation in the visible and infrared range is absorbed in the skin to such a degree so that thermally induced injuries constitute a health hazard. Exposure limits to protect the skin are promulgated on the international level by ICNIRP [1] and in the United States of America in ANSI Z136.1 [2], where they are referred to as the maximum permissible exposure (MPE). The international laser product safety standard IEC 60825-1 [3] also defined MPEs in the annex to protect the skin and to this end adopts the exposure limits as recommended by ICNIRP. Skin-related MPEs are historically based on injury thresholds obtained with porcine models or human volunteers. The discussion in this paper relates to thermally induced skin injury, which is to be distinguished from photochemically induced injury in the ultraviolet range (< 400 nm) [4] and from potential thermo-mechanical injury mechanisms (micro-cavitation around melanosomes) or other non-linear mechanisms for short pulse durations [5].

The injury thresholds, usually expressed as radiant exposure or irradiance, show a strong dependence on wavelength and pulse duration and, to a degree, on the diameter of the laser beam incident on the tissue. While the collection of experimental data covers the parameter range sufficiently to set MPEs, computer models can form the basis for a systematic comparison of injury thresholds with MPEs over a wide range of wavelengths, pulse durations and beam diameters of interest. Of particular interest for such a comparison is the interdependence of trends with wavelength and pulse duration. A number of computer models dedicated to thermal injury of the skin already exist but have been for instance limited to single wavelengths [6,7] or have not been validated against injury threshold levels [8]. However, to the best of our knowledge, none has been validated against in-vivo injury thresholds over a wide range of wavelengths and exposure durations.

The current paper describes in detail a computer model and demonstrates its validity on the basis of a comparison with experimental data in the relevant range of pulse durations longer than 8 µs and wavelengths above 488 nm. An earlier version of the model was presented in 2013 [9]; since then the model has been improved and the experimental database significantly extended. This paper focuses on the systematic review of experimental threshold data and the description and validation of a generalized computer model. An extensive comparison of multiple pulse thresholds against the respective MPE values is discussed in another publication [10]. A detailed

#422618 https://doi.org/10.1364/BOE.422618
Journal © 2021 Received 12 Feb 2021; revised 25 Mar 2021; accepted 30 Mar 2021; published 5 Apr 2021

Biomedical Optics EXPRESS

comparison of computed thresholds with the exposure limits of ICNIRP and ANSI Z136.1 is the topic of another publication [11].

2. Review of bioeffects and experimental data

2.1. Anatomy and physiology

The human skin consists of three main layers. The outermost layer, the epidermis, is a stratified tissue made up to 95% of keratinocytes [12]. The underlying dermis is a heterogeneous assembly of connective tissues – composed among others of collagen and elastic fibers – and including sebaceous glands, hair bulbs and blood capillaries. The hypodermal tissue, referred to as hypodermis or subcutaneous tissue, is essentially made up of fat cells.

Pigmentation of the epidermis originates in the melanocytes, located in the basal part of the epidermis, which produce melanosomes that migrate within the keratinocytes. The thickness of the human epidermis varies amongst different body parts and interdigitates in the dermis (papillae) but it was reported to average between 65 µm and 68 µm on the face, neck and arms [13] and 75 µm on the forearm [14]. The dermis thickness varies between 1 mm and 2 mm depending on the body region [15,16]. Pig skin is a widely accepted model for the human skin with respect to anatomy [13] and response to thermal insult [17,18].

2.2. Nature of the injury

This work is exclusively dedicated to thermally-induced threshold injury of the skin; other interaction mechanisms such as photomechanical damage in the nanosecond regime [19,20] or photochemically induced damage arising from exposure to ultraviolet radiation are not considered. In the thermal regime, absorbed laser energy translates into heat and an injury can occur when critical temperatures are exceeded in the tissue. The mildest reaction to be observed in-vivo by the naked eye is an erythema – often referred to as first-degree burn. On lightly pigmented skin this at-threshold reaction appears as a superficial reddening, while for heavily pigmented skin, skin darkening is observed [21].

In the nanosecond pulse range, several studies report injury thresholds (ED_{50}) for white pig or guinea pig skin significantly lower than in the micro- and millisecond range. At the wavelength of 1314 nm, a ns-pulse ED_{50} of 10.5 J·cm^{-2} was reported, a level up to 8 times lower than ED_{50}s obtained with 600 µs pulses [22]. At 1064 nm, a ns-pulse ED_{50} of 0.7 J·cm^{-2} was reported [20], similar to melanosome thresholds for micro-cavitation [19] and over an order of magnitude lower than ED_{50}s obtained in the µs regime (see Fig. 2(b)), thus suggestive of a photomechanical damage mechanism mediated by the skin pigmentation. At wavelengths approximately longer than 1400 nm, the difference in threshold levels for pulses shorter or longer than 1 µs is less striking, with 3.5 J·cm^{-2} vs. 6.5 J·cm^{-2} at 1540 nm [23], 6.1 J·cm^{-2} vs. 7.4 J·cm^{-2} at 1540 nm [24] or 0.51 J·cm^{-2} vs. 0.97 J·cm^{-2} at 10.6 µm [25] for pulse durations shorter than 1 µs vs. longer than 1 µs, respectively. The latter observations, along with the fact that the role of melanin decreases with increasing wavelength, raise the question whether or not nanosecond-pulse ED_{50}s at wavelengths above approximately 1400 nm are purely thermal in nature, so that a bulk thermal model would also apply. However, injury thresholds obtained with ns-pulses were not further considered in this paper.

2.3. Endpoint for threshold studies

Studies conducted to support the setting of exposure limits need to be based on the determination of the exposure level that just results in a minimum erythemal reaction (or minimum visible lesion, MVL), referred to as threshold lesion. The common endpoint for such studies is the detection of a MVL by direct visual observation at a defined delay after the exposure, such as 1 hour or 24 hours after exposure. Skin thresholds as used for this validation are exclusively

Biomedical Optics EXPRESS

based on visual observation by the un-aided eye to determine if a lesion is formed; other types of assessment such as the examination of biopsies, were not considered, and are also extremely rare when it comes to determination of thresholds.

A threshold is usually defined as the dose having a 50% probability of resulting in a visible lesion and is referred to as the ED_{50}. An in-depth discussion on the meaning of the ED_{50} level and in laser injury experiments can be found in Ref. [26]. The ED_{50} can be obtained by probit analysis of the yes/no injury data [27]. Alternatively to a probit analysis, an injury threshold level can be obtained by bracketing responsive and non-responsive exposure levels, i.e. by consecutively decreasing the exposure from the side where a lesion is detected and increasing the exposure from the side where no lesion is detected – a technique which, however, lends itself only for short delays for the lesion detection [26]. There is no evidence that the results obtained with these two methods differ significantly when applied to skin threshold injuries. However, probit analysis offers some advantages, such as the possibility to quantify the steepness of the tissue response expressed by the ratio of ED_{84} to ED_{50}, commonly referred to as slope of the dose-response curve. For the identified experimental data that were obtained by probit analysis, the median slope was 1.19 (150 samples, maximum slope 2.23), which corresponds to a standard deviation of ±17%, thus indicating a rather steep dose-response curve as compared to other bioeffects or tissues. Noticeably, the average ratio of lowest exposure level leading to an observable lesion to the ED_{50} level was 0.74 (13 samples, minimum ratio 0.30). In the remainder of the paper, the symbol ED_{50} is used even for the case that the threshold was determined by bracketing and not by probit analysis.

Near-threshold lesions evolve in the course of 48 hours. A near-threshold lesion typically appears within few minutes and tends to resolve within a few days [28]. Endpoints are typically 1 h and 24 h, a time course over which one could expect the ED_{50} to change the least. An analysis of experimental studies where the ED_{50}s were reported at different endpoints shows that the 1 h to 24 h ED_{50} ratio on average is close to 1 (see Fig. 1). However, subgroups of the data show the ED_{50}s at 1 h 30% to 65% higher than the ED_{50}s at 24 h [24,29] as well as 30% to 33% lower [23,30], respectively. The different ratios could not be related to either pigmentation, exposure duration, wavelength, spot size or optical penetration depth.

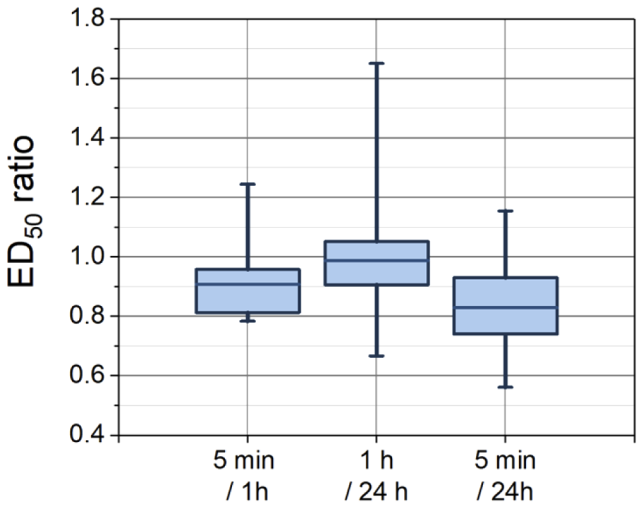

Fig. 1. Ratio of experimental ED_{50}s taken at different endpoints (for references, see section 2.4 and Table S1 in Document 1); endpoints between 1 min and 15 min after exposures were pooled together (labelled as 5 min), endpoints at 24 h and 48 h were pooled together (labelled as 24 h).

Biomedical Optics EXPRESS

On average, the difference between ED_{50}s at 5 minutes and 24 h was significant ($p < 0.005$) but not a large difference relative to the typical standard deviation of experimental threshold levels; the average ED_{50} for the 24 hours endpoint was a factor 0.83 of the average ED_{50} for the 5 minute endpoint. The difference between 5 minutes and 1 h ED50 was not significant, and neither was the difference between 1 h and 24 h ($p > 0.1$). From this analysis it was concluded that the ED_{50} for all endpoints could be pooled to be jointly used for the validation of the computer model. In other words, it was not necessary to develop different Arrhenius parameters for the different endpoints, nor to base the computer model just on 1 h and 24 h data.

2.4. Experimental thresholds

A literature review was conducted in order to identify all relevant experimental studies that report laser induced injury thresholds *in-vivo* for the skin. A total of 293 experimental injury thresholds were identified; 42 of them conducted with human volunteers and 251 with a porcine model of various breeds (Yorkshire, Sinclair, Hanford, Hampshire, Duroc, Chester, white pig and Yucatan mini-pig). The range of relevant experimental data reached from 488 nm to 10.6 µm in terms of wavelength and from 8 µs to 630 seconds in terms of exposure duration. In order to use a consistent term when referring to a wide temporal regime, such as in plots, "exposure duration" is preferred to "pulse duration" even when that regime includes microsecond pulses. Pulses shorter than 1 µs were not considered due to non-purely thermal damage mechanisms. Pulses shorter than 100 µs were only considered for wavelengths above 1600 nm where the contribution of melanin is marginal, as demonstrated in a study with Yucatan mini-pigs at a wavelength of 2000 nm [31]. The irradiance profile of the laser beam incident on the skin was either Gaussian or "top hat". For the specification of the "diameter" of a Gaussian beam profile, the 1/e irradiance level is consistently used throughout this paper, so that dividing the total power by the area defined by the 1/e diameter results in the peak irradiance of the Gaussian beam profile. The beam diameter incident on the skin ranged from 169 µm to 67 mm. Multiple pulse data with up to 3000 pulses were also identified and included.

The relevant injury thresholds [6,7,8,18,21,23–25,28–53] are listed in Table S1 in Supplement 1 along with the predictions of the computer model in the form of a ratio referred to as R_{ED50}, defined as the ratio of the computer model injury threshold to the experimental ED_{50}. The predicted lesion depth is also given (zero being set as the skin surface). Besides wavelength, exposure duration and beam diameter, the skin type and the presence of hair follicles were distinguished for the purpose of modelling. In Table S1 in Supplement 1, the skin color was divided into three groups: "light" for studies reporting "light", "white" or "pigment free" skin types (e.g. "Caucasian" subjects, Yorkshire or Chester white pigs), "medium" for studies reporting "light to dark", "skin type I to type IV" or "lightly pigmented" skin types (e.g. "Chinese" or "light Negro" subjects or Hanford pigs) and "dark" for studies reporting "pigmented" or "dark" skins (e.g. "dark Negro" subjects, Duroc pigs or Yucatan mini-pigs). In cases where the pigmentation was not explicitly reported, photographs or best judgment were used to determine the category. Hairiness was also classified in two categories: "hairless" for studies reporting either hairless (e.g. anterior forearm) or waxed skin sites and "hairy" otherwise. From a total number of 293 thresholds, 5 were not included in the comparison with the predictions of the computer model, for the following reasons.

Amongst eight injury thresholds obtained with pulsed ruby lasers for various skin types, two data using white porcine models appear to be significantly higher (2.5 x to 3.4 x) than other comparable data, as shown in Fig. 2(a). It is noted that the injury threshold does not depend upon the beam diameter for the respective pulse width regime. The data plotted as "light skin" come from human volunteers and white pigs. While it cannot be excluded that the specimen used to derive the highest thresholds (Chester white pig [44] and white pig [51]) were actually pigment-deficient or far less pigmented than other "light skin" subjects (Caucasian volunteers

Biomedical Optics EXPRESS

[21,44]), it is argued that such inconsistency is detrimental for the purpose of model validation. Furthermore, the two highest ED_{50}s are 24 times higher than ED_{50}s obtained with dark skins (Hampshire/Duroc pigs [44] and heavily pigmented volunteers [21]). Such ratios across skin types have never been reported in any other study nor seen across the database available from the literature. Consequently, the two highest ED_{50}s were discarded.

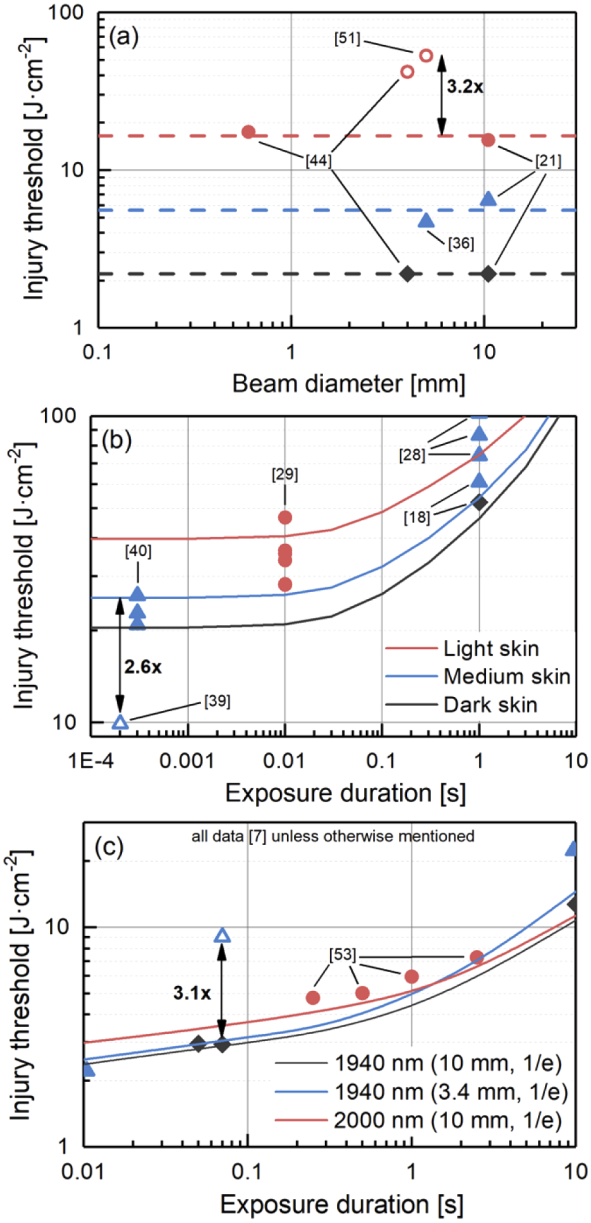

Fig. 2. In-vivo ED_{50}s obtained with (a) pulsed ruby laser for various skin types and highlighting the inconsistency of two data (b) Nd:YAG laser for various skin types along with the respective model predictions and highlighting the inconsistency of a datum at 200 µs and (c) 1940 nm laser radiation on light-skinned porcine models along with the respective model predictions and highlighting the inconsistency of a 70 ms datum.

Biomedical Optics EXPRESS

The injury threshold for pulsed Nd:YAG (200 µs, 1060 nm) on Chinese volunteers reported by Qingshen [39] was 2.6 times lower than the ED_{50} reported in a similar study [40] (9.9 J cm^{-2} vs 26.0 J cm^{-2}). Since laser wavelength, pulse duration, beam diameter, skin type and endpoint (5 minutes) were identical, it is argued that one of the two thresholds must be considered as inconsistent with the overall collection of thresholds. The in-vivo ED_{50}s plotted in Fig. 2(b) (endpoint within 5 minutes, 1060 nm, 5 mm beam diameter, Chinese test subjects) together with the proposed model tend to support the view that the data by Qingshen (9.9 J cm^{-2}) is inconsistent and shall be consequently ignored. Furthermore, the above mentioned article also reports an even lower preliminary ED_{50} obtained with a white pig model (Shanghai white pig, 4.6 J cm^{-2}). That a light skin ED_{50} lies a factor of 2 below that of a pigmented skin is not consistent with biophysical principles, further justifying the rejection of this 1060-nm study for the purpose of model validation.

Finally, the Oliver study of 2010 with a wavelength of 1940 nm [7] contains one inconsistent threshold as shown in Fig.2c. The ED_{50} obtained for a 70 ms exposure and 4.8 mm beam ($1/e^2$) is 3.1 times higher than other data at comparable exposure durations. It is noted that the injury threshold does not depend on the beam diameter for such relatively short exposures at 1940 nm. Since these data all originate from the same study, it can be argued that no uncontrolled parameter (or unreported parameter) could justify such deviation. Consequently, the 1-h and 24-h ED_{50}s (4.8 mm, 70 ms) were not considered in the process of model validation.

3. Description of the computer model

3.1. Optical properties

The skin is a turbid media, for which reflectance is dominated by backscattering in the visible and IR-A (700 nm to 1400 nm) range and specular reflection at longer wavelengths. It has been demonstrated that the melanin content is the dominating parameter when quantifying the diffuse reflectance [21,54] as shown in Fig. 3. Rockwell's data obtained for "Caucasian" and "light Negro" skin types were used in our model for "light" and "medium/dark" skins, respectively.

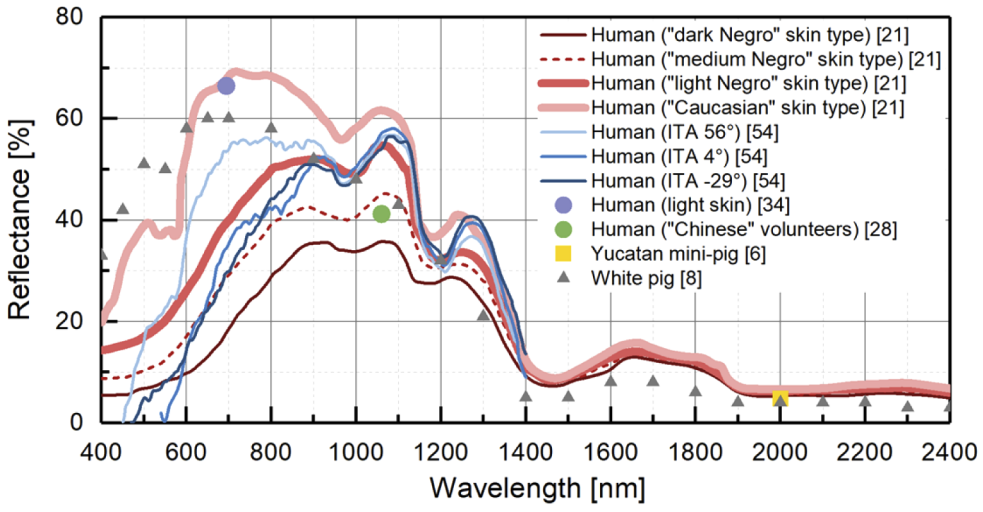

Fig. 3. Diffuse reflectance of various skin types as a function of wavelength found in the literature for human and pig skin.

Scattering in skin tissue has been identified as predominant over absorption in the visible and near infrared [55,56] and certain computer models have implemented light propagation models

Biomedical Optics EXPRESS

using Monte Carlo techniques (e.g. [43]). The proposed model considers attenuation within the different skin layers to be exclusively governed by linear absorption. The attenuation of irradiance E as a function of depth z due to absorption was modelled according to the Beer-Lambert's law:

$$E(z) = (1 - R)E(0)e^{-\alpha \cdot z} \quad (1)$$

where R represents the reflectance and the depth z equals zero at the outer surface of the skin. A combination of four absorbers (melanin, water, blood and fat) at different concentrations in three skin layers (epidermis, dermis and subcutaneous fat) were considered in this model. All pigments are assumed to be homogeneously distributed in their respective layers. The data are summarized in Fig. 4 and Table 1 listing absorption coefficients. In spectral regions where no data are available, the coefficients were set to 0 (blood above 1250 nm and fat above 2600 nm). The layer properties are summarized in Table 2. Epidermis thickness and the volume fraction of the different absorbers were adjusted in the course of an optimization process in order to improve the computer model predictions compared to experimental injury thresholds.

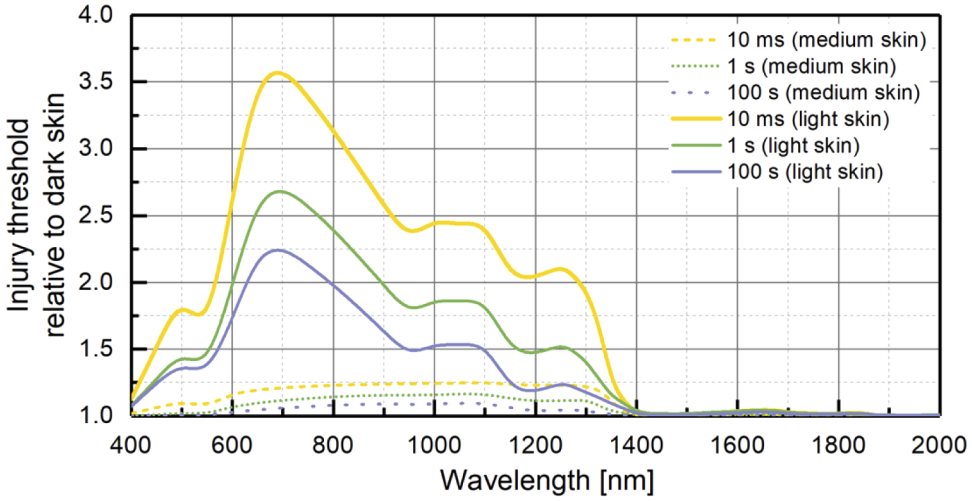

Fig. 4. Absorption coefficient of melanin [57], blood [58], water [59] (data available until 10.6 µm and beyond) and fat [60,61] (data available up to 2600 nm).

Table 1. Bulk absorption coefficients of skin constituents (wavelength λ in nm); see Fig. 4 for water and fat

Constituent	Absorption coefficient α (cm^{-1})	Comments
Melanin	$3.85 \cdot 10^{14}\ \lambda^{-4.2}$	Applicable range: 400 nm to 20 µm; Adopted from [57]
Blood	$1.4040 \cdot 10^{7}$ exp(-0.024 λ) + 2160 exp[-0.0055(417- λ)^2] + 244 exp[-0.0022(542- λ)^2] + 253 exp[-0.0065(577- λ)^2] + 7 exp[-0.00004(920- λ)^2]	Applicable range: 400 nm to 1250 nm; Fit of [58]

3.2. *Transient increase in temperature*

A time-dependent thermal model was developed using a finite-element Multiphysics package (COMSOL 3.5a, Comsol AB, Stockholm, Sweden, 2008), with three contiguous flat slabs representing the epidermis, dermis, subcutis. All layers exhibit homogeneous and isotropic properties. Axial symmetry of the laser beam (either Gaussian or Top Hat) and the irradiated

Biomedical Optics EXPRESS

Table 2. Optical properties of the skin layers; concentrations are volume fractions ("l" for light, "m" for medium and "d" for dark skin)

Parameter	Epidermis	Dermis	Subcutis	Comments
Thickness	120	1000	3000	Unit: µm
Concentration				
Melanin	0.07 (l), 0.095 (m), 0.12 (d)	0.025	0	+25% melanin in the epidermis if hair follicles are present
Water	0.28	1	0.5	
Blood	0.5	0.1	0	
Fat	0	0.2	0.5	

local skin area reduces the problem to a 2D case. The extent of the finite-element domains, both radially and in depth, was set to allow sufficient heat diffusion, i.e. varying with exposure duration and penetration depth. The boundary conditions were adiabatic, except at the air-skin interface where heat losses were accounted for by non-linear boundary conditions. The equation to be solved can be written in the form of the Penne's bio-heat equation:

$$\rho C \frac{\partial T}{\partial t} = k\,\nabla^2 T\; + Q - S_{aq} \tag{2}$$

where *T(t,r,z)* is the increase in temperature, *Q(t,r,z)* represents the heat source (laser radiation) and S_{aq} the heat sink in the tissue. The parameters k, ρ and C are conductivity, density and heat capacity, respectively. The time, radial and axial variables are noted t, r and z, respectively. Heat losses occurring in the dermis via blood flow were taken into account in the bio-heat equation as a negative heat source (heat sink). Besides heat conduction, convection was considered in the dermis via a negative heat source (heat sink) representing the blood flow. Such heat loss can be inserted in the bio-heat equation as a perfusion term $\rho{\cdot}C{\cdot}\omega{\cdot}(T_b\text{-T})$, ω being the perfusion rate and T_b the body temperature. The boundary conditions were as follows:

$$\begin{cases} air - skin : -k\frac{\partial T}{\partial z} = \sigma\varepsilon(T^4 - {T_a}^4) + h(T - T_a) + e(T - T_a)^n \\ elsewhere : -k\frac{\partial T}{\partial z} = 0 \end{cases} \tag{3}$$

where the heat flux at the air-skin boundary depends on a differential between surface temperature T and ambient temperature T_a (both in Kelvin). The first term represents the contribution of radiative heat loss (σ and ε being the Stefan-Boltzmann constant and the emissivity of the skin, respectively), the second term the contribution of free convection with h as heat convection coefficient. A third arbitrary term containing a scaling factor e and an exponent n was introduced to facilitate optimization. The values used for all parameters discussed above are summarized in Table 3, including references, if applicable. Values annotated as "optimized" were adjusted so as to minimize the spread of R_{ED50} ratios (ratio of computer model injury thresholds to experimental ED_{50}).

3.3. Damage model

A thermally-induced threshold injury can be conceptualized as an accumulation of microscopic sub-lethal damage [64], which eventually leads to cell death by apoptosis or necrosis [65]. Such pathway can be modelled by using the Arrhenius equation which describes the temperature-dependent rate of reaction κ and when integrated over time results in a measure of macroscopic

Biomedical Optics EXPRESS

Table 3. List of parameters used in the thermal model

Parameter	Symbol	Unit	Value	Comments
Density	ρ	$kg \cdot m^3$	992	Ref. [62] (water at 40°C)
Conductivity	k	$W \cdot m^{-1} \cdot K^{-1}$	0.63	Ref. [62] (water at 40°C)
Specific heat	C	$J \cdot kg^{-1} \cdot K^{-1}$	4178	Ref. [62] (water at 40°C)
Initial temperature	T_0	K	307	Adapted from Ref. [53] (34°C)
Ambient temperature	T_a	K	295	Arbitrary (22°C)
Blood perfusion rate	ω	s^{-1}	0	Optimized
Emissivity	ε	-	0.975	Adopted from [63]
Convection coefficient	h	$W \cdot m^{-2} \cdot K^{-1}$	15	Adopted from [6]
Scaling factor	e	$W \cdot m^{-2} \cdot K^{-2}$	12	Adopted from [63]
Temperature exponent	n	-	2	Adopted from [63]

damage:

$$\begin{cases} rate : \kappa(t) = A\exp[-E/RT(t)] \\ damage : \Omega = \int_0^\tau \kappa(t)\, dt \end{cases} \quad (4)$$

where *T(t)* is the solution of the heat equation (unit: K) and *R* the ideal gas constant. The parameter *E* is related to an activation energy of the reaction (energy barrier to overcome for the reaction to take place) and the parameter *A* represents the rate of reaction. For a valuable review of the concept of Arrhenius integral and its application to thermal insult see Ref. [66]. The output of the computer model, i.e. the injury threshold, is the lowest exposure level that leads to $\Omega = 1$ within the epidermis or dermis and for a given lesion diameter; this predicted injury threshold can be directly compared to experimental ED_{50} values. The reference point for calculating the damage integral was set to a radial distance of 400 µm from the beam axis, which is equivalent to a minimum visible lesion diameter of 800 µm. The depth at which the lesion first occurs within the skin is not predefined, but is automatically detected by an algorithm. Whenever the peak temperature exceeds 100 °C at threshold level according to the Arrhenius integral ($\Omega = 1$), the damage model was replaced by capping the peak temperature to 100 °C. That is, the Arrhenius integral was not calculated and the threshold is defined as the irradiance level for which the peak temperature reaches exactly 100 °C within the tissue. The results reported in Table S1 in Supplement 1 show that the threshold lesion can occur at various depths depending on the exposure parameters. The Arrhenius parameters used in the damage model are listed in Table 4. Values annotated as "adapted" were adjusted iteratively so as to reduce the spread of R_{ED50}s.

Table 4. List of parameters associated used in the damage model

Parameter	Symbol	Unit	Value	Comments
Activation rate	A	s^{-1}	$8.75 \cdot 10^{82}$	Adapted from Ref. [57]
Activation energy	E	$J \cdot mol^{-1}$	$5.24 \cdot 10^5$	Adapted from Ref. [57]
Lesion diameter	-	µm	800	Optimized

4. Model validation

The computer model described in section 3 was used to reproduce injury thresholds for those wavelengths, exposure durations and laser beam diameters for which relevant experimental threshold data is available, according to section 2 (288 data). The main figure of merit used to evaluate the validity of the computer model was the ratio R_{ED50}, defined as the ratio of computer

Biomedical Optics EXPRESS

model injury threshold to experimental ED_{50} (see Table S1 in Supplement 1). Thus for $R_{ED50} > 1$, the predictions of the computer model can be interpreted as potentially to err on the unsafe side. Further figures of merit such as the trend of R_{ED50} with different laser parameters, animal models or assessment delays were also investigated to confirm the general validity of the computer model. Figure 5 shows the distribution of ratios R_{ED50} with a mean value of 1.01 and the standard deviation of 46%, as listed in Table 5, together with other relevant descriptive statistics. The distribution of R_{ED50}s is close to a normal distribution with a coefficient of determination of 0.92.

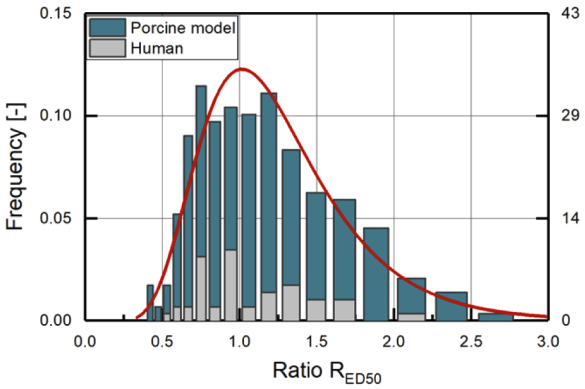

Fig. 5. Distribution of R_{ED50} ratios for the human and pig models (bars), split into bins of constant size on log scale; also shown is a normal distribution with identical average and standard deviation (solid line).

Table 5. Descriptive statistics of the R_{ED50} ratios.

Parameter	Symbol	Value
Number of samples	N	288
Geometric mean	μ	1.01
Standard deviation	σ	46%
Minimum R_{ED50}	-	0.41
Maximum R_{ED50}	-	2.62
Samples within $\mu \pm \sigma$	-	65%
Coefficient of determination	r^2	0.92

The individual R_{ED50}s can also be illustrated as function of exposure duration, wavelength and beam diameter (Fig. 6). No trend indicative of a systematic deviation of the model predictions with a laser parameter was found. It can be seen that the ratios R_{ED50} are approximately evenly distributed around a value of 1 regardless of the laser parameter under consideration. However, it is noted that the computer model overestimates experimental ED_{50}s at the wavelength of 1540 nm, for which the R_{ED50}s on average were found to be significantly different from R_{ED50}s at any other wavelength ($p < 0.01$). These data originate from three studies [23,24,45] and have the pig model and the laser source (pulsed Er:glass laser) in common and encompass a wide range of beam diameters (400 µm to 10 mm) and multiple-pulse exposures with up to 64 pulses, but no single parameter was found that could explain the discrepancy at 1540 nm.

Finally, a number of discrete variables were identified to further analyze the performance of the computer model: the endpoint (categorized as “5 min” for endpoints within 15 minutes after exposure, “1 h” for endpoints at 1 h or 2 h and “24 h” for endpoints at 24 h or 48 h), the species (pig or human), the pigmentation (“light”, “medium” or “dark”, more details in section 2.4), the

Biomedical Optics EXPRESS

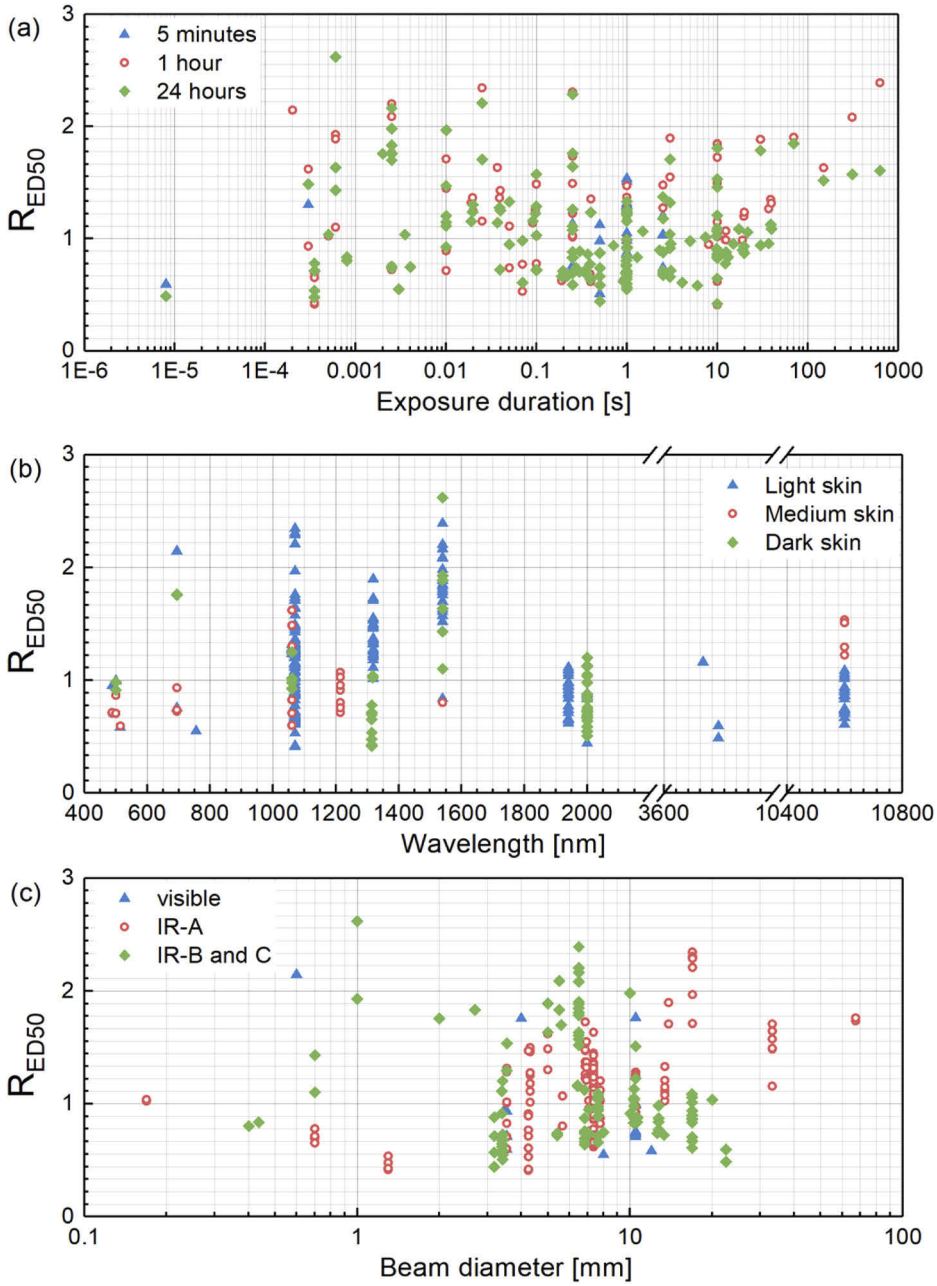

Fig. 6. Distribution of individual R_{ED50} ratios as a function of (a) exposure duration, (b) wavelength and (c) beam diameter (1/e definition); to provide further information, the data in each diagram is split in (a) endpoint at 15 min or less, 1h/2h, 24h/48h after exposure, (b) skin types "light", "medium" or "dark" (c) wavelength below 780 nm, between 780 nm and 1400 nm (IR-A) or above 1400 nm (IR-B or C).

Biomedical Optics EXPRESS

method used to derive a threshold level ("probit" for probit analysis or "other"), the exposure type ("single pulse" or "multiple pulses"), the lesion depth predicted by the computer model ("epidermis" or "dermis") and the presence of hair follicles ("hairless, depilated" or not). A two-tailed unpaired t-test was used to evaluate the geometric mean of R_{ED50}s between groups, the results of which are summarized in Table 6. The t-test was performed for unequal variances whenever the ratio of variances between groups was smaller than 0.5 or greater than 2.

Table 6. Statistical comparison for various variables of interest divided into two groups (threshold for statistical significance: 0.05 level, N.S. means non-significant, the number of samples for each group is given in parentheses; X_{AB} represents the variance of group A over the variance of group B)

Variable	Group A	Group B	X_{AB}	*p-value*
	5 min (30)	1 h (97)	0.52	N.S.
Endpoint	1 h (97)	24 h (161)	1.24	N.S
	5 min (30)	24 h (161)	0.64	N.S.
	Light (208)	Medium (30)	1.65	0.05
Skin type	Medium (30)	Dark (50)	0.51	N.S.
	Light (208)	Dark (50)	0.85	< 0.01
Species	Human (44)	Pig (244)	0.70	N.S.
Technique	Probit (274)	Other (14)	0.81	0.01
Hair follicles[a]	Yes (127)	No (52)	1.74	N.S.
Pulses	Single (213)	Multiple (75)	1.21	N.S.
Lesion depth	Epidermis (194)	Dermis (94)	0.67	0.02

[a]exposures at wavelength < 1400 nm only

5. Discussion

Over the entire range of laser parameters for which laser-induced threshold injuries of the skin are available in the thermal regime, the largest deviation of our computer model predictions to the "unsafe" side, i.e. where model predictions are higher than experimental results, was $R_{ED50} = 2.62$. The maximum deviation to the other side, i.e. where the model threshold predictions are lower than the experimental data, was similar with $R_{ED50} = 0.41$.

Although the endpoints at 5 min and 24h/48h in experimental ED_{50}s were significantly different (see Fig. 1), the average ratio was only 0.83 and therefore negligible as compared to the overall spread of R_{ED50}s. Moreover, the statistics of Table 6 suggests that it is not necessary to differentiate between endpoints. As mentioned in section 2.3, this further demonstrates that the wide range of ratios observed between different endpoints in experimental studies is not reproducible, i.e. cannot be accounted for in simulations, and result in an irreducible deviation of the computer predictions from the *in-vivo* data.

However, it was important to distinguish between different pigment concentrations. The choice of accounting for three skin types in the computer model arose from the wide variety of skin types used in in-vivo studies. As shown in Fig. 7, the predicted injury threshold can vary by as much as 3.6 depending on the skin pigmentation. The difference relates primarily to the reflectance (see wavelength dependence in Fig. 3) and to a lesser degree to the relative contribution of melanin in terms of absorption. This data also demonstrates the challenge for the development of computer models on the basis of in-vivo ED_{50}s, since the categorization of skin types and degree of pigmentation in most published works could be qualified as rough. In the absence of a more meaningful classification scheme quantifying the pigmentation such as the Fitzpatrick's scale, the model must assume a certain pigmentation and its respective properties for each ED_{50} to be reproduced. It is hypothesized that a large part of the R_{ED50} spread is related

Biomedical Optics EXPRESS

to the coarse skin types. The computer model was best in line with the experimental ED_{50}s for melanin concentrations in the epidermis of 7%, 9.5% and 12% for light, medium and dark skin, respectively. Volume fractions reported in the literature vary fairly, with 1% in pale skin to 5% in darker skin [67], 2.5% to 20% for skin type II and skin type IV respectively [68] or an average of 3.8% in light-skinned adults to 30.5% for darkly pigmented skin [69].

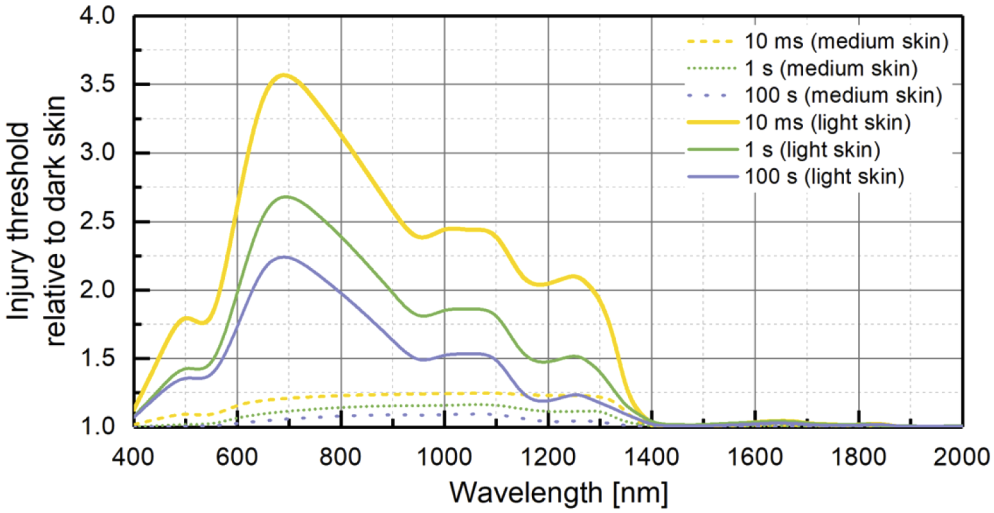

Fig. 7. Change in injury threshold for various skin types according to the computer model, as a function of wavelength and for selected exposure durations.

Similarly to the skin type, the presence or absence of hair follicles was determined to be an important parameter in determining injury thresholds, as shown by DeLisi [30] where lightly pigmented waxed pigs required up to 2.5 times higher irradiance levels to induce a visible lesion than shaved pigs (10 ms, 1070 nm). The difference becomes less important for longer exposure durations and becomes negligible for exposures above 1 s. It was chosen to increase the melanin concentration in the epidermis in this model by 25% to account for the presence of hair follicles. The individual R_{ED50}s are plotted as a function of predicted lesion depth according to the proposed model in Fig. 8. It appears that the computer model overestimates experimental ED_{50}s in the presence of hair follicles for deeply penetrating wavelengths (see R_{ED50}s Fig. 8(a) for lesion depths beyond 120 µm). It also appears that the highest deviations and a majority of R_{ED50}s larger than 2 actually relate to the single wavelength of 1540 nm (see Fig. 8(b)). Although hair takes root in the dermis, attempts to increase the pigmentation in this layer to simulate hair follicles have resulted in a larger spread of the R_{ED50} ratios (data not shown). Any attempted modification of the content of the dermis (e.g. volume fraction of water) or the epidermis thickness also failed to improve the overall deviation. The question remains as to whether the discrepancy is due to the presence of hair follicles, to an optical property of the skin specific to wavelengths around 1540 nm that is not accounted for in the model, or to the properties of the Er:glass lasers used in these studies (e.g. pulse shape or beam profile).

Overall, considering the range of wavelengths, pulse durations, beam diameters, skin types and endpoints, it is argued that the computer model predicts cutaneous injury thresholds relatively well. A significant part of the R_{ED50} spread has been shown to relate to the coarse categorization of skin pigmentation, divided into three types whereas skin colors of the porcine model and human volunteers cover a continuous spectrum from the lightest to the darkest hues. The spread of R_{ED50}s can be assumed to arise to a significant degree from experimental uncertainties. Besides the inherent difficulty to visually infer a threshold lesion appearing as a slight contrast on the skin

Biomedical Optics EXPRESS

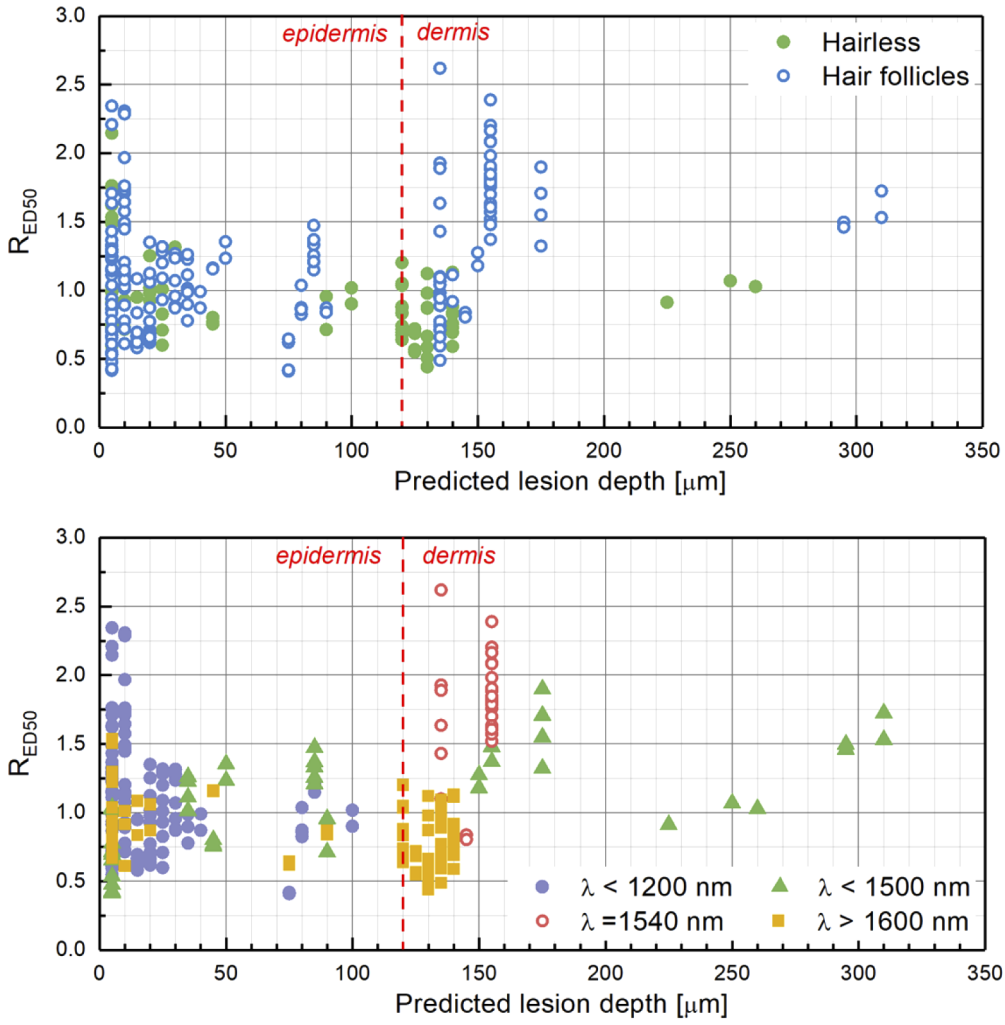

Fig. 8. Predicted lesion depth according to the model, distinguishing (a) between the presence or absence of hair follicles and (b) between four wavelength ranges.

surface (this being even more difficult on dark skins [21]), experimental work providing ED_{50}s for different beam diameters provide a good example of the uncertainty inherent to the in-vivo study of laser-tissue interactions, since for sufficiently short exposure durations, thermal confinement dictates that the injury thresholds do not depend on the beam diameter. The ED_{50}s shown in Fig. 9 for two exposure durations from the same study [29] suggest an experimental uncertainty of a factor 1.5 to 2. The authors of this particular study mention that the short exposures (10 ms) with beams smaller than 10 mm may have been multifocal and lesions at thresholds showed signs of desiccation.

The results also permit the conclusion that a homogenous bulk model is appropriate and it is not necessary to consider the granular aspect of the skin pigmentation for pulse durations above 100 μs, and even shorter durations at wavelengths at which melanin is transparent (above approximately 2000 nm).

Additionally, the use of light propagation models in turbid media to accurately simulate the scattering does not appear to be essential for the purpose of predicting injury thresholds in the

Biomedical Optics EXPRESS

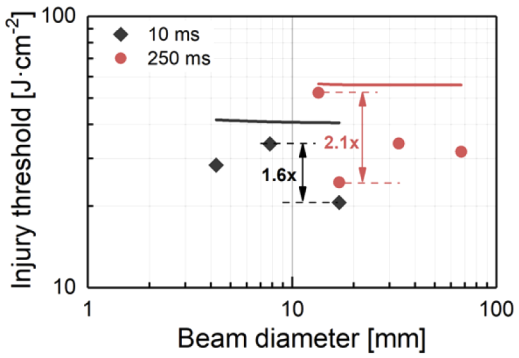

Fig. 9. Comparison of ED_{50}s obtained for lightly-pigmented porcine models [29] (symbols) and model predictions (solid lines) as a function of beam diameter at a wavelength of 1070 nm highlighting the variability of experimental data in a pulse duration range where no spot-size dependence is to be expected.

thermal regime. Although scattering in the skin has been consistently reported in the literature to play a much bigger role in the laser attenuation than the linear absorption, the lack of discernable trend in the performance of this computer model over a wide range of beam diameters – namely 0.8 mm to 67 mm at the 1/e irradiance point – shows that injury thresholds can be predicted well by using the incident beam diameter as the diameter of the heat source within the tissue. Only for beam diameters smaller than 800 µm the heat source in the model was set to a diameter of 800 µm throughout the tissue. This adjustment, in combination with the MVL parameter, was necessary to fit the respective ED_{50}s and can be seen as accounting for scattering in the model for small laser beam diameters. Transmittance measurements have shown that the impact of scattering is significantly greater for small beams than large beams [70]. If it were necessary to account for scattering for beam diameters above 800 µm, a systematic bias of the R_{ED50}s would be seen in the results shown in Fig. 6(c). It is hypothesized that the enlargement of the laser beam within the tissue due to scattering is not significant enough to impact the injury thresholds and that for beam diameters above about 800 µm, the incident beam diameter provides a sufficiently good measure of the radial extent of the heat source.

Additionally to the Arrhenius integral evaluated at the edge of a thin disk referred to as MVL area, a threshold criterion was based on the peak temperature in the beam axis reaching 100 °C. This alternate injury threshold criterion is relevant to exposures associated with small beams (typically less than 1 mm in diameter) and short exposures (typically less than a few milliseconds) where the Arrhenius integral would calculate a peak temperature in the order of 340 K at the MVL radius, while the peak temperature in the beam axis would reach around 400 K. It is argued that such a temperature, even for short times, may result in injuries of a different nature than a superficial erythema (supra-thresholds), especially in the presence of hair follicles. Thermal camera images showed that hair follicles heat over 100°C at exposure levels near ED_{50} while the surrounding skin tissue is associated to temperatures in the order of 40°C [29]. Predicted injury thresholds based on the 100°C criterion were best in line with the experimental ED_{50}s for small beams and short exposures. Without the temperature limitation to 100 °C, additionally to the Arrhenius damage model, these predicted injury thresholds were approximately 40% higher.

Finally, it is noted that the optical properties as discussed in section 3.1 are defined in the wavelength range between 400 nm to 20 µm. Provided that the damage mechanism in the cell is of thermal nature, the predictions of the model can be assumed to be also applicable in the wavelength range of 400 nm to 488 nm and above 10.6 µm where no experimental ED_{50} data is available. In terms of exposure duration, it is suggested not to apply this model to pulses

Biomedical Optics EXPRESS

shorter than 100 µs for wavelengths shorter than approximately 1600 nm and shorter than 1 µs for wavelengths above 1600 nm, where bulk thermal models are not suitable.

6. Conclusion

Compared to the wide parameter range of wavelength, pulse duration, number of pulses, repetition frequency and beam diameter, the collection of experimentally determined skin injury thresholds is somewhat limited. The proposed model was validated to predict thresholds in good agreement with their experimental counterparts, with an overall deviation of 1% and a standard deviation of 46% over a wide range of wavelengths (488 nm to 10.6 µm), exposure durations (8µs to 630 s), beam diameters (0.17 mm to 63 mm) and skin types (light to dark). A validated computer model provides a mean to obtain thresholds in order to cover all combinations of laser parameters relevant to thermal laser-induced injuries and it can be a valuable tool to investigate the suitability of the current laser safety exposure limits and propose potential improvements. An exhaustive comparison of injury thresholds with the current MPEs is the subject of another publication by the authors [11].

Disclosures. The computer model described in this article is used – besides supporting the improvement of international safety limits – to predict skin injury thresholds as part of risk analysis studies for laser applications and products, offered by Seibersdorf Labor GmbH as commercial service.

Supplemental document. See Supplement 1 for supporting content.

References

1. International Commission on Non-Ionizing Radiation Protection, "ICNIRP guidelines on limits of exposure to laser radiation of wavelengths between 180 nm and 1,000 µm," Health Phys. **105**(3), 271–295 (2013).
2. "American National Standard for the safe use of Lasers," Z136.1-2014 (Laser Institute of America).
3. *Safety of Laser Products – Part 1: Equipment Classification and Requirements, IEC 60825-1:2014* (International Electrotechnical Commission, Geneva).
4. D. H. Sliney and M. Wolbarsht, "Safety with lasers and other optical sources," (Publishing Corp., 1980).
5. S.S. Kumru, C. Cain, G. Noojin, M. Imholte, D. Cox, C. Crane, and B. Rockwell, "ED_{50} study of femtosecond terawatt laser pulses on porcine skin," Proc. of SPIE **5695**, 201–208 (2005).
6. B. Chen, S. L. Thomsen, R. J. Thomas, and A. J. Welch, "Modeling thermal damage in skin from 2000-nm laser irradiation," J. Biomed. Opt. **11**(6), 064028 (2006).
7. J. W. Oliver, D. J. Stolarski, G. D. Noojin, H. M. Hodnett, C. A. Harbert, K. J. Schuster, M. F. Foltz, S. S. Kumru, C. P. Cain, C. J. Finkeldei, G. D. Buffington, I. D. Noojin, and R. J. Thomas, "Infrared skin damage thresholds from 1940-nm continuous-wave laser exposures," J. Biomed. Opt. **15**(6), 065008 (2010).
8. A.N. Takata, L. Zaneveld, and W. Richter, "Laser-induced thermal damage of skin," *IIT Research Institute Report for the USAF School of Aerospace Medicine, Chicago IL* (1977).
9. K. Schulmeister and M. Jean, "Computer modeling of laser induced injury of the skin," in *International Laser Safety Conference* (2013), Paper #105.
10. M. Jean, K. Schulmeister, D.J. Lund, and B.E. Stuck, "Comparison of cornea and skin multiple pulse injury thresholds with laser MPEs," in *International Laser Safety Conference* (2019), Paper P106.
11. K. Schulmeister and M. Jean, "Comparison of laser induced skin injury thresholds with laser MPEs" to be submitted to Advanced Optical Technologies Advanced Optical Technologies.
12. J.A. McGrath, R. A. J. Eady, and F.M. Pope, "Anatomy and organization of human skin," Chapter 3 in *Rook's Textbook of Dermatology*, seventh edition (Blackwell Science Ltd, 2004).
13. T. A. Eggleston, W. P. Roach, M. A. Mitchell, K. Smith, D. Oler, and T. E. Johnson, "Comparison of two porcine skin models for *in-vivo* near-infrared laser exposure," Comp. Med. **50**(4), 391–397 (2000).
14. J. Sandby-Møller, T. Poulsen, and H. C. Wulf, "Epidermal thickness at different body sites: relationship to age, gender, pigmentation, blood content, skin type and smoking habits," Acta Derm.-Venereol. **83**(6), 410–413 (2003).
15. H. Alexander and D. L. Miller, "Determining skin thickness with pulsed ultra sound," J. Invest. Dermatol. **72**(1), 17–19 (1979).
16. K. Chopra, D. Calva, M. Sosin, K. K. Tadisina, A. Banda, C. De La Cruz, M. R. Chaudhry, T. Legesse, C. B. Drachenberg, P. N. Manson, and M. R. Christy, "A comprehensive examination of topographic thickness of skin in the human face," Aesthetic Surg. J. **35**(8), 1007–1013 (2015).
17. A.R. Moritz and F.C. Henriques Jr., "Studies of thermal injury: II. The relative importance of time and surface temperature in the causation of cutaneous burns," Am. J. Pathol. **23**(5), 695–720 (1947).
18. M. Baozhang, X. Weiya, Z. Ruipeng, J. Lanying, L. Zhaozhang, and W. Jianu, "Study of injury threshold of CW Nd:YAG laser light for human skin," Chin. J. Lasers **12**, 582–585 (1985).

Biomedical Optics EXPRESS

19. M. S. Schmidt, P. K. Kennedy, G. D. Noojin, R. L. Vincelette, R. J. Thomas, and B. A. Rockwell, "Trends in nanosecond melanosome microcavitation up to 1540 nm," J. Biomed. Opt. **20**(9), 095011 (2015).
20. M.P. DeLisi, A.M. Peterson, G.D. Noojin, A.D. Shingledecker, A.J. Tijerina, A.R. Boretsky, M.S. Schmidt, S.S. Kumru, and R.J. Thomas, "Porcine skin damage thresholds for pulsed nanosecond-scale laser exposure at 1064-nm," Proc. SPIE **10492**, 1049207 (2018).
21. R.J. Rockwell Jr. and L. Goldman, "Research on human skin laser damage thresholds," *Report DERM-LL-74-1003, USAF School of Aerospace Medicine, Brooks Air Force Base TX* (1974).
22. C.P. Cain, W.P. Roach, D.J. Stolarski, G.D. Noojin, S.S. Kumru, K.L. Stockton, J.J. Zohner, and B.A. Rockwell, "Infrared laser damage thresholds for skin at wavelengths from 0.810 to 1.54 microns for femtosecond to microsecond pulse durations," Proc. of SPIE **6435**, 64350W (2007).
23. A.V. Lukashev, B.I. Denker, P.P. Pashinin, and S.E. Sverchkov, "Laser damage of skin by 1540 nm Er-glass laser radiation. Impact to laser safety standards," Proc. of SPIE **2965**, 22–32 (1996).
24. C. P. Cain, G. D. Polhamus, W. P. Roach, D. J. Stolarski, K. J. Schuster, K. L. Stockton, B. A. Rockwell, B. Chen, and A. J. Welch, "Porcine skin visible lesion thresholds for near-infrared lasers including modeling at two pulse durations and spot sizes," J. Biomed. Opt. **11**(4), 041109 (2006).
25. A.S. Brownell and B.E. Stuck, "Corneal and skin hazards of CO_2 laser radiation," *Proc. of ninth Army Science Conference*, 123–137 (West Point, 1974).
26. D. H. Sliney, J. Mellerio, V. P. Gabel, and K. Schulmeister, "What is the meaning of threshold in laser injury experiments? Implications for human exposure limits," Health Phys. **82**(3), 335–347 (2002).
27. B.J. Lund, "The Probitfit program to analyze data from laser damage threshold studies," Report WTR/06-001, Walter Reed Army Institute of Research, Washington DC (2006).
28. W. Tingbi, L. Yunong, X. Yupeng, and C. Mingzai, "Study on the damage threshold of human skin caused by continuous YAG laser," Chin. J. Lasers **12**, 626–628 (1985).
29. R. Vincelette, G. D. Noojin, C. A. Harbert, K. J. Schuster, A. D. Shingledecker, D. Stolarski, S. S. Kumru, and J. W. Oliver, "Porcine skin damage thresholds for 0.6 to 9.5 cm beam diameters from 1070-nm continuous-wave infrared laser radiation," J. Biomed. Opt. **19**(03), 1 (2014).
30. M. P. DeLisi, M. S. Schmidt, A. F. Hoffman, A. M. Peterson, G. D. Noojin, A. D. Shingledecker, A. R. Boretsky, D. J. Stolarski, S. S. Kumru, and R. J. Thomas, "Thermal damage thresholds for multiple-pulse porcine skin laser exposures at 1070 nm," Proc. SPIE **25**(3), 035001 (2019).
31. B. Chen, D. C. O'Dell, S. L. Thomsen, R. J. Thomas, and A. J. Welch, "Effect of pigmentation density upon 2.0 mm laser irradiation thermal response," Health Phys. **93**(4), 273–278 (2007).
32. A.C. Bostick, T.E. Johnson, D.Q. Randolph, and G.C. Winston, "Response of pigmented porcine skin (sus scrofa domestica) to single 3.8 micron laser radiation pulses," Proc. of SPIE **5686**, 668–673 (2005).
33. A. S. Brownell, W. H. Parr, and D. K. Hysell, "Skin and carbon dioxide laser radiation," Arch. Environ. Health **18**(3), 437–442 (1969).
34. A.S. Brownell. D.K. Hysell and W.H. Parr, "Millisecond exposure of porcine skin to simulated CO_2 laser radiation," *US Army Medical Research Laboratory, Report no. 953, Fort Knox KY* (1971).
35. B. Chen, J. Oliver, R. Vincelette, G. Pocock, R. Zaman, and A.J. Welch, "Porcine skin ED_{50} damage thresholds for 1214 nm laser irradiation," Proc. of SPIE **6854**, 685406 (2008).
36. C. Ji, W. Jun, L. Shanfen, X. Guidao, S. Liangshun, Q. Huanwen, and W. Denglong, "Injury threshold of ruby laser irradiation on human skin," *Chin. J. Lasers* 12 (1985).
37. S. Hongmin, L. Jishi, T. Yankang, L. Panxiang, C. Zhongben, X. Xingbing, and Y. Yuehuan, "Acute injury threshold level of CO_2 laser light for skin of yellow race," *Chin. J. Lasers* 12 (1985).
38. L. Jishi, S. Hongmin, T. Yankang, L. Panxiang, and C. Zhongben, "Measurement of erythematous reaction by argon laser light for skin of yellow race," *Chin. J. Lasers* 12 (1985).
39. W. Qingshen, D. Peiying, Z. Ruipong, H. Qingshen, G. Baokang, J. Lanying, and W. Jianu, "Investigation on laser injury threshold of skin," *Chin. J. Lasers* 12 (1985).
40. W. Tingbi, L. Yunong, X. Yupeng, and C. Mingzai, "Study on the damage threshold of human skin caused by 300 microsecond pulsed neodymium glass laser," Chin. J. Lasers **12**, 628–630 (1985).
41. T. E. Johnson, B. K. Ketzenberger, K. B. Pletcher, S. P. Wild, and W. P. Roach, "Skin exposures from 1318 nm laser pulses," Proc. of SPIE **4257**, 355–362 (2001).
42. C. I. Montes de Oca, C. P. Cain, K. Schuster, K. Stockton, J. J. Thomas, T. A. Eggleston, and W. P. Roach, "Measured skin damage thresholds for 1314 nm laser exposures," Proc. of SPIE **4953**, 117–123 (2003).
43. J. W. Oliver, R. Vincelette, G. D. Noojin, C. D. Clark, C. A. Harbert, K. J. Schuster, A. D. Shingledecker, S. S. Kumru, J. Maughan, N. Kitzis, G. D. Buffington, D. J. Stolarski, and R. J. Thomas, "Infrared skin damage thresholds from 1319-nm continuous-wave laser exposures," J. Biomed. Opt. **18**(12), 125002 (2013).
44. W.H. Parr, "Skin lesion threshold values for laser radiation as compared with safety standards," *US Army Medical Research Laboratory, Report no. 813, Fort Knox KY* (1969).
45. P. J. Rico, T. E. Johnson, M. A. Mitchell, B. H. Saladino, and W. P. Roach, "Median effective dose determination and histologic characterization of porcine (Sus scrofa domestica) dermal lesions induced by 1540-nm laser radiation pulses," Comp. Med. **50**(6), 633–638 (2000).
46. G. Simon, P. Schmid, W. G. Reifenrath, T. van Ravenswaay, and B. E. Stuck, "Wound healing after laser injury to skin – The effect of occlusion and vitamin E," J. Pharm. Sci. **83**(8), 1101–1106 (1994).

Biomedical Optics EXPRESS

47. D. Tata, V.I. Villavicencio, M.C. Cook, T.E. Dayton, C.D. Clark, C.A. Moreno, J.A. Ross, J.S. Eggers, P. Kennedy, D. Christensen, and J. Notabartolo, "Infrared laser induced skin damage and perception," *Air Force Research Laboratory, Report AFRL-HE-BR-TR-2005-0139, Brooks City-Base TX* (2005).
48. W. Verkruysse, W. Jia, W. Franco, T. E. Milner, and J. S. Nelson, "Infrared measurement of human skin temperature to predict the individual maximum safe radiant exposure (IMSRE)," Lasers Surg. Med. **39**(10), 757–766 (2007).
49. L. Jiao, J. Wang, Y. Fan, and Z. Yang, "Porcine skin damage thresholds and histological damage characteristics from 1319-nm laser radiation," J. Biomed. Opt. **24**(09), 1 (2019).
50. L. Jiao, C. Wang, K. Zhang, J. Wang, and Z. Yang, "Porcine skin damage threshold from mid-infrared optical parametric oscillator radiation at 3.743 µm," Biomed. Opt. Express **11**(12), 7165–7174 (2020).
51. C. Ji and L. Shanfen, "Experiment on the damage of pig skin irradiated by ruby laser," Chin. J. Lasers **12**, 631–632 (1985).
52. M.P. DeLisi, K.J. Schuster, G.D. Noojin, A.J. Tijerina, A.D. Shingledecker, M.S. Schmidt, S.S. Kumru, and B.A. Rockwell, "Porcine skin damage thresholds for multiple-pulse laser exposure at 1940nm," Proc. of SPIE **11238**, 112380C (2020).
53. B. Chen, D. C. O'Dell, S. L. Thomsen, B. A. Rockwell, and A. J. Welch, "Porcine skin ED_{50} damage thresholds for 2,000 nm laser irradiation," Lasers Surg. Med. **37**(5), 373–381 (2005).
54. H. Piazena, H. Meffert, and R. Uebelhack, "Spectral remittance and transmittance of visible and infrared-A radiation in human skin – Comparison between *in-vivo* measurements and model calculations," Photochem. Photobiol. **93**(6), 1449–1461 (2017).
55. X. Ma, J. Qing Lu, H. Ding, and X.-H. Hu, "Bulk optical parameters of porcine skin dermis at eight wavelengths from 325 to 1557 nm," Opt. Lett. **30**(4), 412–414 (2005).
56. E. Salomatina, B. Jiang, J. Novak, and A. N. Yaroslavsky, "Optical properties of normal and cancerous human skin in the visible and near-infrared spectral range," J. Biomed. Opt. **11**(6), 064026 (2006).
57. M. Jean and K. Schulmeister, "Validation of a computer model to predict laser induced retinal injury thresholds," J. Laser Appl. **29**(3), 032004 (2017).
58. S. Prahl, https://omlc.ogi.edu/spectra/hemoglobin/ for "Optical absorption of hemoglobin," Last accessed December 28, 2020.
59. D. J. Segelstein, "The complex refractive index of water," M.S. Thesis, University of Missouri-Kansas City, Kansas City, MO (1981).
60. R.L.P. van Veen, H.J.C.M. Sterenborg, A. Pifferi, A. Torricelli, and R. Cubeddu, "Determination of VIS- NIR absorption coefficients of mammalian fat, with time- and spatially resolved diffuse reflectance and transmission spectroscopy," in Biomedical Topical Meeting, OSA Technical Digest, paper SF4 (Optical Society of America, 2004).
61. G.B. Altshuler, R.R. Anderson, and D. Manstein, "Method and apparatus for the selective targeting of lipid-rich tissues," *US patent US 6,605,080 B1* (2003).
62. D. R. Lide, *CRC Handbook of Chemistry and Physics: A Ready-reference Book of Chemical and Physical Data*, 73rd ed. (CRC Press, 1993).
63. M. Jean, K. Schulmeister, D. J. Lund, and B. E. Stuck, "Laser-induced corneal injury: validation of a computer model to predict thresholds," Biomed. Opt. Express **12**(1), 336–353 (2021).
64. J. R. Lepock, "Cellular effects of hyperthermia: relevance to the minimum dose for thermal damage," Int. J. Hyperthermia **19**(3), 252–266 (2003).
65. N. P. Matylevitch, S. T. Schuschereba, J. R. Mata, G. R. Gilligan, D. F. Lawlor, C. W. Goodwin, and P. D. Bowman, "Apoptosis and accidental cell death in cultured human keratinocytes after thermal injury," Am. J. Pathol. **153**(2), 567–577 (1998).
66. S. L. Jacques, "Ratio of entropy to enthalpy in thermal transitions in biological tissues," J. Biomed. Opt. **11**(4), 041108 (2006).
67. T. Lister, P. A. Wright, and P. H. Chappell, "Optical properties of human skin," J. Biomed. Opt. **17**(9), 0909011 (2012).
68. K.P. Nielsen, L. Zhao, J.J. Stamnes, K. Stamnes, and J. Moan, "The optics of human skin: Aspects important for human health," *Solar Radiation and Human Health* 1 (2008).
69. S. L. Jacques, "Origins of tissue optical properties in the UVA, visible, and NIR regions," OSA TOPS on Advances in Optical Imaging and Photon Migration **2**, 364–369 (1996).
70. Z.-Q. Zhao and P.W. Fairchild, "Dependence of light transmission through human skin on incident beam diameter at different wavelengths," Proc. of SPIE **3254**, 354–360 (1998).